

Influence of Annealing on Structure of Nylon 11

Qingxin Zhang, Zhishen Mo,* Siyang Liu, and Hongfang Zhang

State Key Laboratory of Polymer Physics & Chemistry, Changchun Institute of Applied Chemistry, Chinese Academy of Sciences, Changchun 130022, P. R. China

Received February 17, 2000; Revised Manuscript Received May 3, 2000

ABSTRACT: Differential scanning calorimeter (DSC), wide-angle X-ray diffraction (WAXD), small-angle X-ray scattering (SAXS), and density techniques have been used to investigate the structural parameters of the solid state of Nylon 11 annealed at different temperatures. The equilibrium heat of fusion ΔH_m^0 and equilibrium melting temperature T_m^0 were estimated to be 189.05 J g^{-1} and 202.85°C respectively by using the Hoffman–Weeks approach. The degree of crystallinity ($W_{c,x}$) ranged approximately 24–42% was calculated by WAXD and compared with those by calorimetry ($W_{c,h}$) and density ($W_{c,d}$) measurements. The radius of gyration R_g , crystalline thickness L_c , noncrystalline thickness L_a , long period L , semiaxes of the particles (a , b), electron-density difference between the crystalline and noncrystalline regions $\eta_c - \eta_a$, and the invariant Q increased with increasing annealing temperature. The analysis of the SAXS data was based upon the particle characteristic function and the one-dimensional electron-density correlation function. An interphase region existed between the crystalline and noncrystalline region with a clear dimension of about 2 nm for semicrystalline Nylon 11. Instead of the traditional two-phase model, a three-phase model has been proposed to explain these results by means of SAXS.

1. Introduction

In the past decade, many research interests had been devoted to a kind of semicrystalline high performance engineering thermoplastic, Nylon 11, due to its excellent piezoelectricity and mechanical properties. Up to now, the isothermal and nonisothermal crystallization kinetics,¹ crystal structure,² morphology,³ and piezoelectricity⁴ of Nylon 11 have been investigated.

The DSC method has been successfully used to analyze the thermodynamic and kinetic processes and WAXD is a powerful method to study the crystal structure of polymer. SAXS can be used to characterize the parameters of particles over a length range larger than the usual interatomic distances. In this paper, DSC, WAXD, and SAXS measurements were performed to study the solid state of Nylon 11.

On the basis of a lattice theory, Flory⁵ suggested that an interphase region might exist in the lamellae between the crystalline and noncrystalline region of semicrystalline polymers, the properties of which differ from those of a truly noncrystalline region. Wendorff et al.⁶ pointed out that the formation of an interphase region was an intrinsic property of the lamellae within crystalline regions and that such an interphase region must influence the structural and dynamical properties of the polymer. The thickness of the interphase region was predicted to be 1–2 nm.⁵ Comparing the thickness of the interphase region with the thickness of the crystal lamellae indicated that this value is reasonable. Instead of the traditional two-phase model, a three-phase model has been proposed to explain these results by means of SAXS.

In practical production and research, the annealing treatment is a very useful crystallization technique, which is usually applied to accelerate the secondary crystallization process under the temperature of the maximum crystallization rate. To extend the study on WAXD and SAXS technique, our work is focused on the

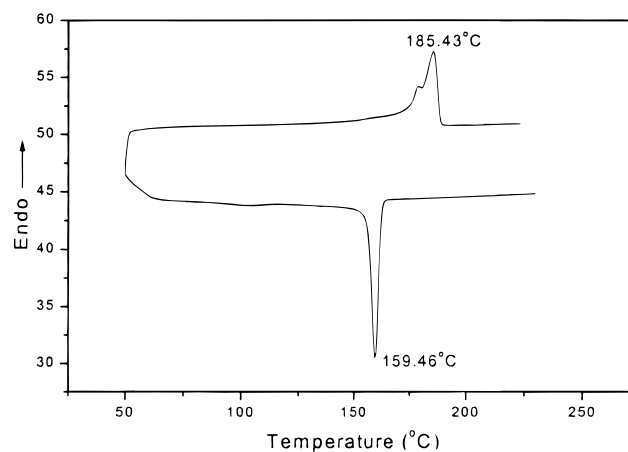
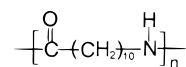


Figure 1. DSC trace of the Nylon 11 sample.

structural parameters of the solid state of Nylon 11 at different annealing temperatures.

2. Experimental Section

2.1. Materials. The samples of Nylon 11 ($M_w = 46\,000 \text{ g mol}^{-1}$) were synthesized by the Changchun Institute of Applied Chemistry from castor oil, which has the following chemical repeating unit:



The DSC trace of Nylon 11 granule is presented in Figure 1, from which the melting point, $T_m = 185.43^\circ\text{C}$, and the melt crystallization temperature $T_c = 159.46^\circ\text{C}$ were obtained (heating and cooling rate = 10°C/min). Nylon 11 samples were fully melted in a molding press at 240°C for 15 min and annealed at different temperatures, T_a in the range of 60 – 185°C for 1 h, then gradually cooled to room temperature.

2.2. Differential Scanning Calorimetry. Equilibrium thermodynamic parameters were determined using a Perkin-Elmer DSC-7 differential scanning calorimeter calibrated the temperature with indium. All DSC experiments were performed under a nitrogen purge; sample weights were between

* Corresponding author

10–11 mg. The samples were heated quickly (at 80 °C/min) to 20–30 °C above the melting temperature (T_m), stayed there for 10 min to eliminate residual crystals, then cooled (at –80 °C/min) to the designated crystallization temperatures (T_c) in the range of 164–172 °C for the isothermal crystallization process.

2.3. Density Measurement. The density of the samples was measured by suspension method in an *n*-heptane/carbon tetrachloride mixed solution using a PZ-B-5 liquid-density balance.

2.4. WAXD. WAXD experiments were performed at room temperature using a Rigaku D/max 3C diffractometer with curved graphite crystal filtered Cu K α_1 radiation ($\lambda = 0.154\ 06$ nm). The observed film specimens were fixed on a rotating sample-stage of the goniometer in order to eliminate the anisotropic effect, so a suitable average of the diffracted intensity in reciprocal space can be obtained. Data were collected from $2\theta = 5$ – 45° in a fixed time mode with a step interval of 0.02° .

2.5. SAXS. SAXS experiments were performed at room temperature using a Philips PW-1700 X-ray diffractometer equipped with a Kratky small-angle X-ray camera, a step-scanning device, and a scintillation counter for recording the scattering intensity. The distance between the sample and detector was 20 cm. The exposure time was 2 h for all the samples investigated. This counting time was long enough to avoid the influence of noise on the scattering intensity, so that during the process of data collection the count error was less than 1% for the largest angle. The scattering intensities were corrected for absorption, background scattering, and incident X-ray fluctuations of the samples. Desmeared scattering intensities were obtained by adopting a procedure developed by Schmidt.⁷ The resulting curves were converted to the absolute scattering intensity using a calibrated Lupolen (Polyethylene, BASF, Ludwigshafen, Germany) standard sample.⁸

3. Results

As a semicrystalline polymer, Nylon 11 can crystallize from the rubbery state at temperatures between 45 and 185 °C. With such a wide range of crystallization temperature, the crystalline morphology of Nylon 11 may be strongly dependent on the thermal treatment, and the resulting changes of morphology from the thermal history influence the mechanical properties of Nylon 11.

3.1. Equilibrium Thermodynamic Parameters. The equilibrium heat of fusion ΔH_m^0 and equilibrium melting temperature T_m^0 are two important thermodynamic parameters characterizing the inter- and intramolecular reactions, and they are of significance in the fabrication and application of polymers, however, the equilibrium values are not available by direct measurement, thus indirect or extrapolation methods must be used.

a. Equilibrium Heat of Fusion, ΔH_m^0 . Nowadays, a number of methods are available to determine ΔH_m^0 of a crystalline polymer.⁹ Among them the approach of extrapolating the linear relationship between the heat of fusion, ΔH_m and the specific volume, V_{sp} of samples with different degrees of crystallinity to the 100% crystalline condition has proved to be successful in the determination of ΔH_m^0 for many linear semicrystalline polymers.^{10,11} Therefore, specimens with different degree of crystallinity were prepared by annealing under different conditions. The heats of fusion (ΔH_m) were determined by DSC and respective specific volumes (V_{sp}) were measured with a density gradient column. Figure 2 shows the plot of ΔH_m against V_{sp} for the differently annealed Nylon 11 samples. Through linear regression,

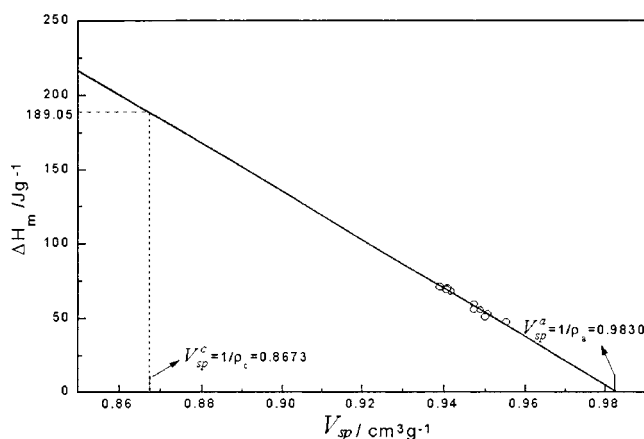


Figure 2. Determination of enthalpy of fusion for fully crystalline Nylon 11 from the relation between specific volume V_{sp} and heat of fusion ΔH_m .

an expression of the form

$$\Delta H_m = 1604.25 - 1631.86 V_{sp} \text{ J g}^{-1} \quad (1)$$

was obtained with a correlation factor $r = -0.996$. If V_{sp}^c (specific volume) of a hypothetical 100% crystalline Nylon 11, i.e., $0.8673 \text{ cm}^3 \text{ g}^{-1}$ as calculated from the unit cell dimension is substituted for V_{sp} , and $\Delta H_m^0 = 189.05 \text{ J g}^{-1}$ is derived.

b. Equilibrium Melting Temperature, T_m^0 . The equilibrium melting temperature T_m^0 is another important macroscopic quantity to characterize a given crystal of a flexible linear macromolecule. As a main approach, the Hoffman–Weeks equation has been widely used to estimate the equilibrium melting point of polymers.

According to theoretical considerations by Hoffman and Weeks,¹² the equilibrium melting point of polymers cannot be measured directly, but can be deduced from DSC measurements by plotting the observed apparent melting temperature T_m vs T_c . The equilibrium melting point is obtained by the intersection to the resulting straight line with the line $T_m = T_c$. Assuming chain folding during crystallization, the dependence of the apparent melting temperature T_m on the crystallization temperature T_c is given by

$$T_m = T_m^0 \left(1 - \frac{1}{2\beta}\right) + T_c \frac{1}{2\beta} \quad (2)$$

where β is the lamellar thickening factor which describes the growth of lamellar thickness during crystallization. Under equilibrium conditions, β is equal to 1. At the higher crystallization temperatures, the slope of plot was 0.5 and extrapolated to a thermodynamic melting point of $T_m^0 = 202.85 \text{ }^\circ\text{C}$ for Nylon 11 (see Figure 3).

3.2. Crystallinity Analysis. a. WAXD Method. The degree of crystallinity, $W_{c,x}$, is given by

$$W_{c,x} = \frac{I_c}{I_c + KI_a} \quad (3)$$

where I_c and I_a are the integrating intensities scattered over a suitable angular interval by the crystalline and the noncrystalline regions, respectively, and K is a calibration constant. If the sample is anisotropic, a suitable average of the diffraction intensity in reciprocal space must be obtained.

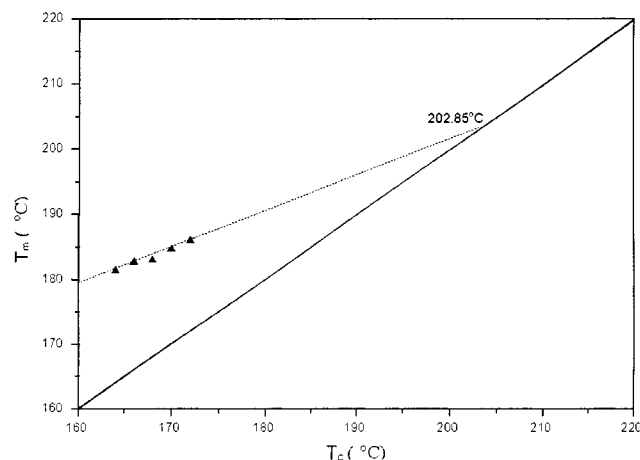


Figure 3. Application of Hoffman-Weeks approach to Nylon 11 for determining its equilibrium melting temperature T_m^0 .

By means of the graphic multippeak resolution method,¹³ the degree of crystallinity determined by WAXD is calculated as follows

$$W_{c,x} = \frac{\sum_i C_{i,hkl}(\theta) I_{i,hkl}(\theta)}{\sum_i C_{i,hkl}(\theta) I_{i,hkl}(\theta) + k_i C_a(\theta) I_a(\theta)} \quad (4)$$

where $I_{i,hkl}(\theta)$ = relative intensities of the crystalline peaks, $I_a(\theta)$ = relative intensity of the noncrystalline peak; $C_{i,hkl}(\theta)$ = correction factors of crystalline peaks; $C_a(\theta)$ = correction factor of noncrystalline peak; the total correction factor $K = C_a(\theta)k_i$, and k_i is the relative scattering coefficient, which is a ratio of calculating diffraction intensity ($\sum I_{i,cal}$) to total scattering intensity ($\sum I_{i,total}$) for unit weight of crystalline polymer $k_i = \sum I_{i,cal} / \sum I_{i,total}$ ($k_i \leq 1$). $C_{i,hkl}(\theta)$ or $C_a(\theta)$ can be calculated by the following equation

$$C_{i,hkl}^{-1} \text{ or } C_a^{-1}(\theta) = \frac{1 + \cos^2 2\theta}{\sin^2 \theta \cos \theta} f_i^2 e^{-2B(\sin \theta / \lambda)^2} = \frac{\sum N_i f_i^2}{\sin^2 \theta \cos \theta} \frac{1 + \cos^2 2\theta}{e^{-2B(\sin \theta / \lambda)^2}} \quad (5)$$

where f = atomic scattering factor of a repeating unit, f_i = scattering factor of the i th atom, N_i = the number of the i th atom in a repeating unit, 2θ = Bragg angle, $(1 + \cos^2 2\theta) / (\sin^2 \theta \cos \theta)$ = angle factor (LP), $e^{-2B(\sin \theta / \lambda)^2}$ = temperature factor (T), and $2B = 10$.

The atomic scattering factor f_i can be approximately expressed by

$$f_i(\sin \theta / \lambda) = \sum_{i=1}^4 a_i e^{-b_i (\sin \theta / \lambda)^2} + c \quad (6)$$

where values of a , b and c are given in ref 14.

WAXD patterns of Nylon 11 annealed at different temperatures show one noncrystalline peak at 20.8° and 12 crystalline peaks including four distinct crystalline peaks at 2θ of 7.5 , 20.0 , 23.5 , and 38.0° (see Figure 4). These four peaks correspond to the (001), (100), (010, 110), and (023) crystal planes, respectively. The relative intensities (relative area) of all the crystal planes were calculated, and the results were shown in Table 1.

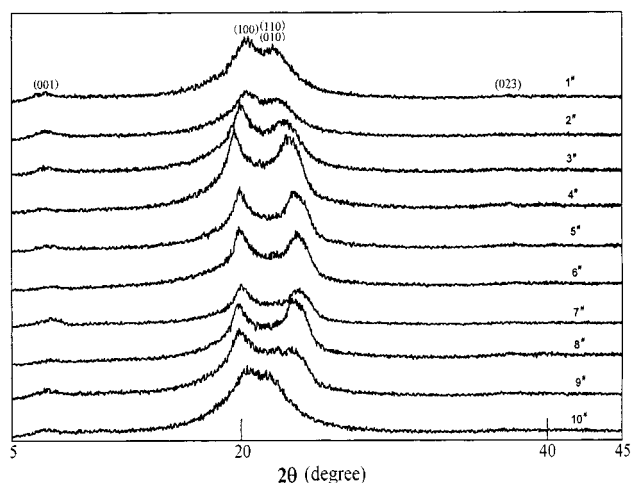


Figure 4. WAXD patterns of Nylon 11 annealed at various temperatures (annealing temperatures shown in Table 2).

Table 1. Indices of Crystallographic Planes and Their Relative Diffraction Intensities of Nylon 11

NO	2θ (deg)	d_{obsd} (nm)	d_{calcd} (nm)	hkl	I/I_0	K_i
1	7.5	1.1777	1.1789	001	16	
2	11.5	0.7688	0.5590	002	12	
3	20	0.4435	0.4340	100	100	
4	23.5	0.3782	0.3748	010	96	
			0.3680	110		
5	38	0.2366	0.2366	023	18	
6	40.5	0.2225	0.2235	022	15	0.724
7	44	0.2025	0.2038	120	15	
8	48.5	0.1875	0.1889	112	12	
9	51.5	0.1773	0.1770	213	10	
10	60.5	0.1529	0.1518	222	7	
			0.1539	232		
11	63	0.1474	0.1477	320	6	
			0.1471	312		
12	66	0.1414	0.1415	301	8	
			0.1414	212		

Table 2. Correction Factors of X-ray Diffraction Peaks for Nylon 11

hkl	2θ (deg)	T	LP	f^2	correction factors
001	7.40	0.9826	477.9	500.77	0.085
100	20.12	0.8793	62.65	361.93	1
010,110	23.16	0.8438	46.80	324.95	1.57
023	37.85	0.6419	16.32	181.74	10.5
A^a	20.85	0.8711	58.17	352.98	1.12

^a Noncrystalline peak.

Using eqs 4–6, the correction factors at formula of the degree of crystallinity for the crystalline and noncrystalline peaks were calculated and listed in Table 2. The correction factors of crystalline peaks are $C_{001}(\theta) = 0.085$, $C_{100}(\theta) = 1$, $C_{010,110}(\theta) = 1.57$, and $C_{023}(\theta) = 10.5$, and the correction factor of the noncrystalline peak is $C_a(\theta) = 1.12$. The total correction factor $K = k_i C_a(\theta) = 0.811$. Using the data above, eq 4 can be further reduced to give eq 7. The $W_{c,x}$ was calculated on the base of eq

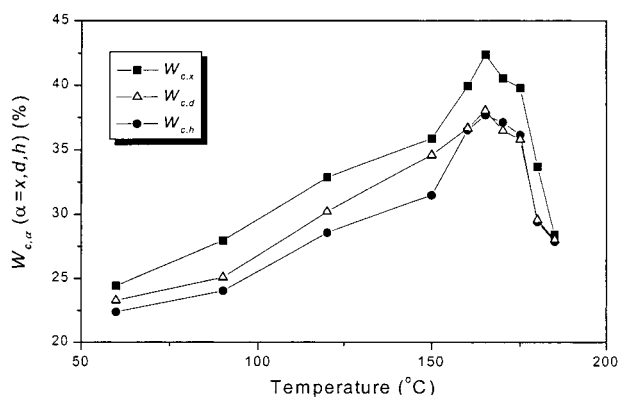
$$W_{c,x} = \frac{0.085 I_{001} + I_{100} + 1.57 I_{010,110} + 10.5 I_{023}}{0.086 I_{001} + I_{100} + 1.57 I_{010,110} + 10.5 I_{023} + 0.811 I_a} \quad (7)$$

7, and the results were listed in Table 3 and shown in Figure 5.

b. Density Method. The degree of crystallinity of the mass fraction from density measurement ($W_{c,d}$) can be

Table 3. Degree of Crystallinity, Density, and Enthalpy of Fusion for Nylon 11

NO	T_a (°C)	ρ_s (g·cm ⁻³)	V_s (cm ³ ·g ⁻¹)	ΔH_m (J·g ⁻¹)	$W_{c,x}$ (%)	$W_{c,d}$ (%)	$W_{c,h}$ (%)
1 [#]	185	1.052	0.9506	52.678	28.42	28.01	27.86
2 [#]	180	1.054	0.9488	55.581	33.69	29.56	29.4
3 [#]	175	1.062	0.9416	68.312	39.77	35.78	36.13
4 [#]	170	1.062	0.9408	70.151	40.53	36.47	37.11
5 [#]	165	1.065	0.9390	71.215	42.37	38.03	37.67
6 [#]	160	1.063	0.9406	69.026	39.94	36.65	36.51
7 [#]	150	1.060	0.9430	59.495	35.85	34.57	31.47
8 [#]	120	1.053	0.9497	53.563	32.86	30.21	28.57
9 [#]	90	1.046	0.9552	47.432	27.96	25.09	24.03
10 [#]	60	1.025	0.9756	44.972	24.42	23.28	22.37

**Figure 5.** Effect of annealing temperature T_a on the degree of crystallinity $W_{c,x}$, $W_{c,d}$, and $W_{c,h}$.

usually calculated by the formula

$$W_{c,d} = \frac{\frac{1}{\rho_a} - \frac{1}{\rho_s}}{\frac{1}{\rho_s} - \frac{1}{\rho_c}} \quad (8)$$

where ρ_a and ρ_c are densities of the noncrystalline and crystalline regions respectively; ρ_s is the sample density. $W_{c,d}$ was calculated on the base of eq 8 and the results were also listed in Table 3 and shown in Figure 5.

c. Calorimetry Method. The degree of crystallinity by calorimetry ($W_{c,h}$) can be calculated by means of the equation

$$W_{c,h} = \frac{\Delta H_m}{\Delta H_m^0} \quad (9)$$

where ΔH_m and ΔH_m^0 are the fusion enthalpies of the sample and the complete crystalline Nylon 11, respectively. On the basis of the eq 9, $W_{c,h}$ was calculated and compared with $W_{c,x}$ and $W_{c,d}$ in Figure 5.

3.3. Coherence Length ξ . The coherence length ξ perpendicular to the (hkl) plane, ξ_{hkl} in nanometers, is usually given by the Scherrer equation^{15,16}

$$\xi_{hkl} = 5.73 \frac{K\lambda}{\beta \cos \theta} \quad (10)$$

where β is pure line broadening and $\beta = (B^2 - b_0^2)^{1/2}$, B is the measured half-width of the experimental profile (in degree), b_0 is the instrumental broadening, which was obtained to be 0.15° from scans of standard silicon powder, K is the Scherrer factor, here $K = 0.9$, λ is the wavelength of the X-ray, and θ is the Bragg angle. Using the data of the four distinct crystalline peaks shown in

Table 4. Coherence Length Perpendicular to the Different Crystal Planes of Nylon 11 Annealed at Different Temperatures

NO	ξ (nm)			
	001	100	010, 110	023
1 [#]	2.18	2.65	2.61	
2 [#]	2.34	3.30	3.26	
3 [#]	2.25	4.04	3.77	2.47
4 [#]	2.95	3.95	3.91	2.81
5 [#]	2.87	3.64	3.78	2.27
6 [#]	2.18	4.35	3.70	2.40
7 [#]	2.28	4.04	3.66	2.63
8 [#]	2.07	3.23	2.90	2.37
9 [#]	2.34	3.11	2.80	
10 [#]	2.18	2.89	2.75	2.47

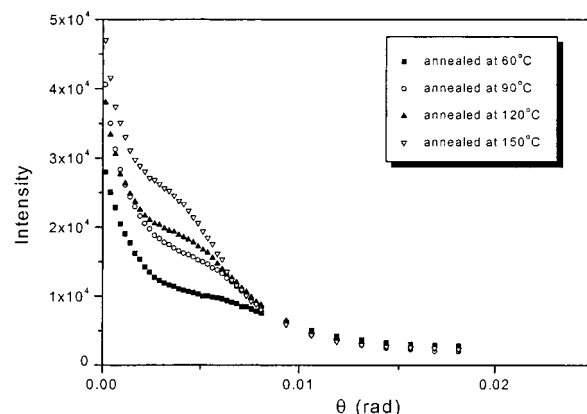
**Figure 6.** SAXS curves of scattering intensity versus scattering angle for Nylon 11 sample annealed at indicated temperatures for 1 h.

Table 1, the coherence length was calculated by eq 10 (see Table 4). The coherence length of (100) plane ξ_{100} is larger than the values of other planes. The reason is that the hydrogen bonds exist in (100) planes, so the molecular chains are easier to move and recrystallize in the (100) planes and the activity energy of the recrystallization process is lower.

3.4. SAXS Analysis. SAXS reflects electron-density fluctuations within a sample over a length range larger than the usual interatomic distances. Semicrystalline Nylon 11, which consists of a simplified two-phase system of alternating crystalline domains and a non-crystalline matrix, could be assumed to be a system with fluctuating electron density, and it should scatter X-rays. The scattering capacity depends on the density difference between the crystalline and noncrystalline regions. The SAXS curves of Nylon 11 annealed at different temperatures (60, 90, 120, and 150 °C) are shown in Figure 6. It could be seen that the scattering intensities increased gradually with increasing T_a .

a. Radius of Gyration. Guinier et al.^{17,18} have shown that the scattering intensity $I(h)$ of the polymer at small angle can be shown with the following equation:

$$I(h) \approx I_e N n^2 e^{-h^2 R_g^2/3} \quad (11)$$

Here, I_e is the scattering intensity of an electron, N is the number of all the irradiated particles, n is the electron number of one particle, $h = 4\pi(\sin \theta)/\lambda$, λ is the wavelength of X-ray, $\theta = \epsilon/2$, ϵ is the scattering angle, and $\epsilon = \arctan(P_i - P_0)/l$, P_i is the scattering highness of the i th point, and P_0 is the beginning scattering height, l is the distance between the sample and the counting instrument, and R_g is the radius of gyration.

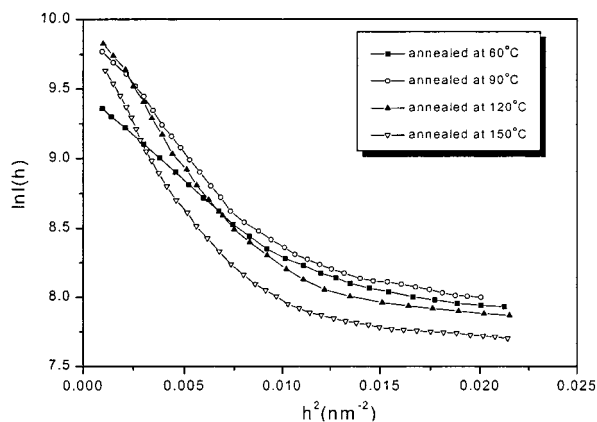


Figure 7. Plots of $\ln(I(h))$ vs h^2 for Nylon 11 annealed at various temperatures.

Table 5. Structural Parameters of the Solid State for Nylon 11 Annealed at Different Temperatures

T_a (°C)	$T_a = 60$ °C	$T_a = 90$ °C	$T_a = 120$ °C	$T_a = 150$ °C
$\rho_c - \rho_a$ (g cm ⁻³)	0.044	0.066	0.086	0.090
R_g (nm)	1.81	1.95	2.29	2.99
$I_e N r^2$	12508.41	19925.06	22754.67	32780.76
a (nm)	2.837	3.055	3.587	4.683
b (nm)	0.536	0.584	0.696	0.913
ω	0.189	0.191	0.194	0.195
S/V_p (m ² cm ⁻³ 10 ⁻³)	1.12	1.47	2.01	2.54
Q (10 ⁻⁴ mol e cm ⁻³)	1.539	1.933	1.831	1.795
$\eta_c - \eta_a$ (mol e cm ⁻³)	0.0328	0.0493	0.0642	0.0672
d (nm)	6.73	6.96	7.07	7.21
L_c (nm)	2.61	3.98	4.14	4.52
L_a (nm)	9.61	8.40	7.32	7.06
d_{tr} (nm)	1.69	1.76	2.27	2.31
L (nm)	15.6	15.9	16.0	16.2

The logarithm form of eq 11 is

$$\ln(I(h)) = -\frac{R_g^2}{3}h^2 + \ln(I_e N r^2) \quad (12)$$

$$= Kh^2 + B$$

where $K = -\frac{R_g^2}{3}$ and $B = \ln(I_e N r^2)$. K is the slope, B is the intercept of $\ln(I(h)) \sim h^2$ curve and $I_e N r^2$ is the intensity coefficient. R_g and $I_e N r^2$ are given by

$$R_g = \sqrt{-3K} \quad (12.1)$$

$$I_e N r^2 = e^B \quad (12.2)$$

The $\ln(I(h)) \sim h^2$ curves will be close to a straight line within the small angle range for all the shapes of particles. This angle range is broader for the sphere particles system than the others, and it will decrease with the particles departing from the spherical shape. Figure 7 shows the plot of $\ln(I(h)) \sim h^2$ of Nylon 11 annealed at different temperatures. The radius of gyration R_g are obtained by the eq 12.1 and shown in Table 5.

b. Characteristic Function $v_0(r)$. If we assume there are two points, that point P exists in one particle, point Q is a random point, and the distance between these two points is r , so the probability of point Q existing in this particle can be defined as the particle

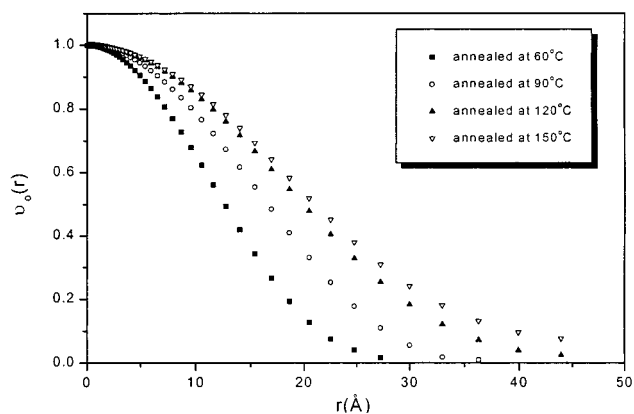


Figure 8. Plots of particle characteristic function $v_0(r)$.

characteristic function $v_0(r)$ and it can be expressed as^{17,19}

$$v_0(r) = \frac{\frac{1}{r} \int_0^\infty h I(h) \sin(hr) dh}{\int_0^\infty h^2 I(h) dh} \quad (13)$$

The following four equations can be draw from eq 13:¹⁷

$$v_0\langle L_c \rangle = 0 \quad (13.1)$$

$$\int_0^\infty v_0(r) dr = \frac{L_c}{2} \quad (13.2)$$

$$\int_0^\infty 4\pi^2 v_0(r) dr = V_p \quad (13.3)$$

$$\left[\frac{d(v_0(r))}{dr} \right]_{r=0} = -\frac{S_0}{4V_p} \quad (13.4)$$

Here V_p is the volume of the particle, L_c is the crystalline thickness, S_0 is the surface area of the particle, and S_0/V_p is the specific surface area.

The characteristic function $v_0(r)$ of Nylon 11 annealed at different temperatures is shown in Figure 8. As we have discussed above, respectively, the crystalline thickness L_c and the specific surface area S_0/V_p can be obtained from the integral area of $v_0(r) \sim r$ curves and the slope of $v_0(r)$ curves when r approaches 0. To find the semiaxes of the ellipsoid (a , b), the experimental curve $v_0(r)$ was compared with a series of simulative curves with the different values of axial ratio ω ($= b/a$) but the same radius of gyration, then the analogous one must be got and the axial ratio can be determined. The semiaxes (a , b) can be calculated by

$$a = R_g \left(\frac{5}{\omega^2 + 2} \right)^{1/2} \quad (14)$$

$$b = \omega a \quad (15)$$

The specific surface area S_0/V_p , semiaxes (a , b) of the ellipsoid particles and the crystalline thickness L_c are obtained (see Table 5).

c. One-Dimensional Electron Density Correlation Function $K(Z)$. If the variation of the electron density obeys a "linear model", i.e., the density variations mainly occur along the direction perpendicular to the lamellae, then, to describe the structural change of

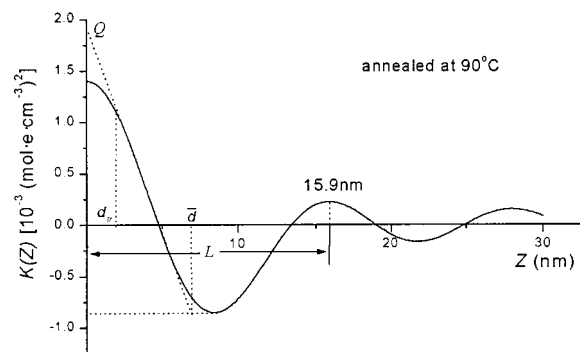


Figure 9. Curve of experimental correlation function $K(Z)$ obtained for Nylon 11 annealed at 90 °C.

the system, we can use the 1D EDCF (one-dimensional electron density correlation function). The correlation function $K(Z)$ can be written as^{20,21}

$$K(Z) = \langle [\eta(Z) - \langle \eta \rangle][\eta(Z + Z) - \langle \eta \rangle] \rangle \quad (16)$$

where Z is the direction normal to lamellar stacks and the angular brackets indicate averaging over all coordinates Z within a representative stack which will pass through a noncrystalline layer and a crystalline layer. The average electron density within the stack is called $\langle \eta \rangle$. $K(Z)$ can be obtained by Fourier transformation of the desmeared scattering intensities

$$K(Z) = 4\pi \int_0^\infty s^2 I(s) \cos(2\pi sZ) ds \quad (17)$$

where $s = 2(\sin \theta)/\lambda$. As an example, the derived typical 1D EDCF $K(Z)$ of the lamellar structure for Nylon 11 annealed at 90 °C is demonstrated in Figure 9. From the well-known “self-correlation triangle” which reflects the electron-density correlation within a lamella, one can directly estimate various structural parameters of the solid state for Nylon 11 by making use of some general properties of the correlation function. The invariant Q is the value of $K(Z)$ at $Z = 0$ which is also evaluated by extrapolating the straight-line section of the self-correlation region to the $K(Z)$ axis (see Figure 9). Its physical meaning is the mean-square electron-density fluctuation, which could satisfactorily explain the changing tendency of the values of Q considering the variation of the electron-density difference with the annealing temperature. The long period L could be determined from the position of the first maximum in the correlation function. The average lamellar thickness \bar{d} can be obtained by the cross point of the baseline with the sloping line of the “self-correlation triangle”.

Buchanan²² proposed a two-phase model consisting of an infinite array of alternating crystalline and noncrystalline regions. From the traditional “ideal two-phase model”, the self-correlation section of the SAXS curve was expected to be a straight line. As we employed a simplified two-phase model to analyze the SAXS data, the long period L should be expressed as $L = L_c + L_a$; here, L_c and L_a are the thickness of crystal and the noncrystalline regions, respectively. In fact, the deviation is usually observed in practical results, indicating that the boundary between the crystalline and noncrystalline regions are not clear and sharp and there exists a transition zone^{23–25} (interphase region) with a finite width instead of a sharp jump in density. From the curvature of the straight-line segment in the central section of $K(Z)$, the thickness of the transition layer d_{tr}

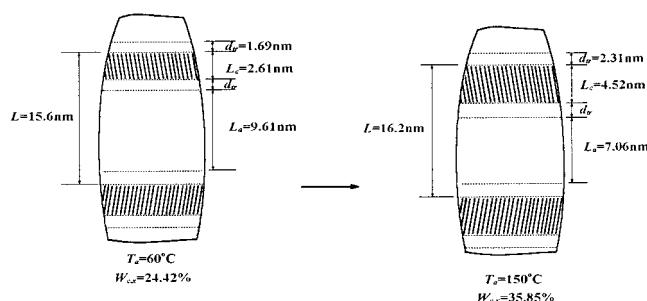


Figure 10. Schematic representation of the bimodal microstructure of Nylon 11 annealed at different temperature.

could be estimated. The most important difference between the two- and three-phase models is that the latter possesses a transition zone between the noncrystalline layer and the crystalline layer. According to Strobl,²⁰ the thickness of the transition zone d_{tr} can be directly derived from the curvature of $K(Z)$.

The thickness of the transition layer d_{tr} was given by the lower limit of the straight section in the self-correlation range. The noncrystalline thickness L_a can be calculated from

$$L = L_a + 2d_{tr} + L_c \quad (18)$$

The result of long period L , noncrystalline thickness L_a , invariant Q , average lamellar thickness \bar{d} , and thickness of transition layer d_{tr} are obtained and listed in Table 5. Schematic representations of the three-phase structure of Nylon 11 with different crystallinities are shown in Figure 10.

4. Discussion

4.1. Influence of Annealing on the Degree of Crystallinity. The values of $W_{c,\alpha}$ ($\alpha = x, d, h$) for every sample exhibit a similar distribution with the change of T_a . No matter which measurement method was used, the values of $W_{c,\alpha}$, which range approximately from 24 to 42%, first increase and then decrease with increasing annealing temperature. The annealing treatment probably enhanced the growth of secondary crystallization which had a lower melting point than that of the major lamellae with a higher one. With the increase of annealing temperature, the degree of crystallinity of Nylon 11 systematically increased and more perfect crystals were formed because of the rearrangement of the molecular chains and the improvement of the regularity of the chains between the major lamellae. It was the above-mentioned effect that made the secondary crystallization during the large lamellae undergo a reorganization and perfection process. There is a maximum value of the crystallinity around 165 °C, indicating that there exists an optimum annealing temperature in the proximity of this temperature. The reason the values of $W_{c,x}$ for the specimens annealed at high temperature decrease with the increasing temperature is partly that unstable and small crystals melt and transform into the noncrystalline region, although more perfect crystallites are favorably formed at higher temperature. So, the total amount of crystallinity reduces and the degree of crystallinity for the samples slowly cooled from the melt decreases.

Figure 5 shows that the results of the degree of crystallinity calculated from WAXD are compatible with those from density and calorimetry measurements and the values of the degree of crystallinity exhibit the

following order $W_{c,x} > W_{c,d} > W_{c,h}$. The crystalline, interphase and the noncrystalline regions contribute to WAXD, density and calorimetry methods to different degree. $W_{c,x}$ is equal to the sum of the content of crystalline and interphase regions, and $W_{c,d}$ is calculated by the difference of packing density between the crystalline and noncrystalline regions, while the $W_{c,h}$ is obtained only by the enthalpy of crystalline region fusion. Moreover, various techniques are affected to different extents by imperfections and interfacial effects. Therefore, some disagreement among the quantitative results of the degree of crystallinity by different measurement methods is frequently encountered.²⁶

4.2. Influence of Annealing on Structure Parameters. The above discussions revealed that the degree of crystallinity ($W_{c,x}$), sample densities (ρ_s) and crystal densities (ρ_c) are all influenced by the annealing temperature (see Table 3). Taking into account the variability of the crystal densities with the annealing temperature, the density difference between the crystalline and noncrystalline regions $\Delta\rho = \rho_c - \rho_a$ is not constant (see Table 5). Moreover, we can also find the semiaxis b is very much less than a , which means the particles grow mainly in the two-dimensional direction.

Nylon 11 is such a kind of polymer which crystallizes very quickly, but the degree of crystallinity is usually very low while it is cooled from the melt. When its glassy state was annealed above T_g (45 °C), with an increase of T_a , the moving ability of the molecular chains increases and some of the disordered molecular chains in the noncrystalline region moved and rearranged into the interphase or crystalline region. Meanwhile, the molecular chains of the interphase region moved and arranged more orderly than before. The results of long period L , crystalline thickness L_c , and the thickness of transition layer d_{tr} all increase with the increase of the annealing temperature except the noncrystalline thickness L_a . A conclusion can be drawn that the molecular chains in the transition zone move and form a crystal easier than the chains in the noncrystalline region because the crystalline thickness L_c increases more obviously than d_{tr} . Namely, the activation energy between the crystalline region and transition zone is lower than that between the noncrystalline and the transition zone.

5. Conclusion

The degree of crystallinity ($W_{c,x}$) is calculated by WAXD and compared with those calorimetry ($W_{c,h}$) and density ($W_{c,d}$) measurements, moreover, the value of degree of crystallinity values exhibit the following order: $W_{c,x} > W_{c,d} > W_{c,h}$. There is a maximum value of the degree of crystallinity around 165 °C, indicating that there is an optimum annealing temperature for Nylon 11. With increase of the annealing temperature, the radius of gyration R_g , crystalline thickness L_c , the

semiaxes of the particles (a , b), long period L , electron-density difference between the crystalline and noncrystalline regions $\eta_c - \eta_a$ and the invariant Q all increase except the thickness of noncrystalline region L_a . Moreover, the semiaxis b is less than a very much, which means the particles grow mainly on the two-dimensional direction. The results also indicate that a transition zone exists between the traditional "two phases" with a clear dimension of about 2 nm.

Acknowledgment. This work was supported by the National Natural Science Foundation of China (No. 59873023) and subsidized by Special Funds for Major State Basic Research Projects.

References and Notes

- (1) Liu, S. Y.; Yu, Y. N.; Cui, Y.; Zhang, H. F.; Mo, Z. S. *J. Appl. Polym. Sci.* **1998**, *70*, 2371.
- (2) Yoshiyuki, T.; Masataka, T.; Masayuki, K.; Takeo, F. *Polym. J.* **1997**, *29*(3), 234.
- (3) Balizer, E.; Fedderly, D.; Haught, D.; Dickens, B.; Deroggi, A. S. *J. Polym. Sci., Part B: Polym. Phys.* **1994**, *32*, 365.
- (4) Takase, Y.; Lee, J. W.; Scheinbeim, J. I.; Newman, B. A. *Macromolecules* **1991**, *24*, 6644.
- (5) Flory, P. J.; Yoon, D. Y.; Dill, K. A. *Macromolecules* **1984**, *17*, 862.
- (6) Hahn, B. R.; Herrmann-Schönherr, O.; Wendorff, J. H. *Polymer* **1987**, *28*, 201.
- (7) Schmidt, P. W. *Acta Crystallogr.* **1965**, *19*, 938.
- (8) Kratky, I.; Pilz, I.; Schmitz, P. J. *J. Colloid Interface Sci.* **1966**, *21*, 24.
- (9) Wunderlich, B. *Macromolecular Physics*; Academic Press: New York, 1980.
- (10) Harberkorn, H.; Illers, K. *Polym. Sci.* **1979**, *257*, 820.
- (11) Mo, Z. S.; Meng, Q. B.; Feng, J. H.; Zhang, H. F.; Chen, D. L. *Polym. Int.* **1993**, *32*, 53.
- (12) Hoffman, J. D.; Weeks, J. J. *J. Chem. Phys.* **1962**, *37*, 1723.
- (13) Mo, Z. S.; Zhang, H. F. *J. Macromol. Sci.—Rev. Macromol. Chem. Phys.* **1995**, *C35*, 555.
- (14) *International Tables for X-ray Crystallography*; The Kynoch Press: Birmingham, England, 1974.
- (15) Liu, T. X.; Mo, Z. H.; Wang, S. E.; Zhang, H. F. *Macromol. Rapid Commun.* **1997**, *18*, 23.
- (16) Mo, Z. S.; Lee, K.-B.; Moon, Y. B.; Kobayashi, M.; Heeger, A. J.; Wudl, F. *Macromolecules* **1985**, *18*, 1972.
- (17) Guinier, A.; Fournet, G. *Small-Angle Scattering of X-rays*; Wiley: New York, 1955.
- (18) Wu, T. W.; Speapen, F. *Acta Metall.* **1985**, *33*, 2185.
- (19) Meng, Z. F. *Acta Sci. Nat. Univ. Jilin* **1989**, *3*, 67.
- (20) Strobl, G. R.; Schneider, M. *J. Polym. Sci., Polym. Phys. Ed.* **1980**, *18*, 1343.
- (21) Debye, P.; Bueche, A. *J. Appl. Phys.* **1949**, *20*, 518.
- (22) Buchanan, D. R.; McCullough, R. L.; Miller, R. L. *Acta Crystallogr.* **1968**, *20*, 922.
- (23) Mandelkern, L.; Alamo, R. G.; Kennedy, M. A. *Macromolecules* **1990**, *23*, 4721.
- (24) Zhang, H. F.; Yang, B. Q.; Zhang, L. H.; Mo, Z. S. *Macromol. Chem. Phys.* **1996**, *197*, 553.
- (25) Könke, U.; Zachmann, H. G.; Baltá-Calleja, F. J. *Macromolecules* **1996**, *29*, 6019.
- (26) Glotin, M.; Mandelkern, L. *Colloid. Polym. Sci.* **1982**, *260*, 182.

MA000298D